Controlled Lateral Pressure on Cortical Bone Using Blade-Equipped Implants. An Experimental Study in Rabbits

Vitor Ferreira Balan , Mauro Ferri , Eduardo Pires Godoy , Leticia Gabriela Artioli , Daniele Botticelli * , Erick Ricardo Silva , Samuel Porfirio Xavier

Posted Date: 9 July 2024

doi: 10.20944/preprints202407.0788.v1

Keywords: animal study; bone healing; histology; cortical layer; marginal gap

Article

Controlled Lateral Pressure on Cortical Bone Using Blade-Equipped Implants. An Experimental Study in Rabbits

Vitor Ferreira Balan [1], Mauro Ferri [2], Eduardo Pires Godoy [3], Leticia Gabriela Artioli [1], Daniele Botticelli [4*], Erick Ricardo Silva [1], Samuel Porfirio Xavier [1]

[1] Department of Oral and Maxillofacial Surgery and Periodontology, University of São Paulo, Faculty of Dentistry of Ribeirão Preto, Av. do Café - Subsetor Oeste - 11 (N-11), Ribeirão Preto - SP, 14040-904, Brazil. V.F.B., vitor.balan@usp.br; (E.R.S.) erick.silva@usp.br, (L.G.A.), leticia.artioli@usp.br, (S.P.X.) spx@forp.usp.br
[2] Private Practice, 130001 Cartagena de Indias, Colombia. (M.F.) medicina2000ctg@hotmail.com
[3] Department of Basic and Oral Biology, University of São Paulo, Ribeirão Preto School of Dentistry. (E.P.G.), eduardo.godoy@usp.br
[4] ARDEC Academy, 47923 – Rimini, Italy (D.B.) daniele.botticelli@gmail.com
* Correspondence: daniele.botticelli@gmail.com

Abstract: Background: This study stands as a pioneer in the histological evaluation of the biological behavior of a novel implant design featuring decompressive cervical blades. Hence, the aim of the present study was to evaluate the healing outcome in cortical regions at where decompressive protocols were adopted using implants equipped with blades. Materials and methods: Blades with varying diameters were integrated into the coronal portion of the implant to prepare the cortical region of rabbit tibiae. The blade diameters differed from the implant collar by the following amounts: control group (0 μm), +50 μm, and +200 μm. Results: No marginal bone loss was detected. Instead, all implants exhibited new bone formation in the coronal region. Complete closure was observed in the CG-0 group, as well as in the TG-50 and TG-200 groups, despite the presence of marginal gaps without primary bone contact at installation. In the apical region, most implants breached the cortical layer. Nevertheless, new bone formation in this region completely closed the osteotomy, effectively isolating the internal environment of the tibia from the external. Conclusions: The use of a blade attached to the implant body enabled precise preparation of the cortical layer, allowing for controlled decompression in the targeted area. This technique resulted in optimal osseointegration with no loss of marginal bone, and complete restoration of marginal gaps ranging from 0 μm to 200 μm.

Keywords: animal study; bone healing; histology; cortical layer; marginal gap

1. Introduction

Osseointegrated implants are extensively employed in esthetic and functional restorations for individuals affected by partial or total edentulism. Recent research indicates that titanium possesses properties that promote interaction with the surrounding bone tissue [1,2], giving implants mechanical characteristics suitable for withstanding the demands of masticatory loads and physiological stimuli during the chewing process [3].

Despite the significant success rates documented with implants, a variety of studies have been conducted with the aim of optimizing osseointegration through the application of different technologies and manufacturing methods. These innovations focus on modifying the surface microtopography [4–8] through physicochemical means and the design of implants with respect to macrogeometry [9–11]. Preclinical studies demonstrate that these alterations significantly improve the biological performance of implants [12–14].

Bone compression during the installation of integrated bone implants plays a fundamental role in the primary stability of the implant [15], however excessive compressions can induce distortions in the peri-implant bone, resulting in adverse effects on local microcirculation and increasing the risk

 doi:10.20944/preprints202407.0788.v1

of bone necrosis, leading to implant failure [16,17]. Additionally, compressive insertions may also be associated with pain and resorption of the bone crest adjacent to the implants [18–20].

Recent research suggests that reduced levels of bone compression around the implant are associated with increased osseointegration [21–23]. Therefore, it is crucial that an ideal implant is designed to maintain an appropriate balance between tensile and compressive forces [24]. Furthermore, it has been observed that high insertion torques can lead to increased bone compression around implants, resulting in significant marginal bone resorption and subsequent implant failure [25].

It was further shown that modifying the macrogeometry of implants by incorporating a decompression chamber in the threads resulted in an improvement in the osseointegration process. [26,27].

For experimental investigations of the interaction between implants and bone tissue, as well as to assess the impact of implant macrogeometry on new bone formation, the animal model using rabbit tibia is widely utilized [28]. The tibia of these animals presents notable distinctions in topographic and morphological aspects, as it can be divided into two well-defined regions: the diaphysis, characterized by the presence of cortical bone and a medullary space, resembling type II bone; and the metaphysis, composed of trabecular tissue resembling type III bone. The variation in bone morphology and density between these two regions is related to the amount of bone formation occurring in each of them [29–32].

Although there are studies that assess the impact of decompression chambers on new bone formation around bicortical implants inserted into rabbit tibia, investigations into bone behavior around implants containing decompressive cervical blades under similar conditions have not been investigated sufficiently yet.

Therefore, this study stands as a pioneer in the histological evaluation of the biological behavior of a novel implant design featuring decompressive cervical blades. Hence, the aim of the present study was to evaluate the healing outcome in cortical regions at where decompressive protocols were adopted using implants equipped with blades.

2. Materials and Methods

2.1. Ethical statements

The protocol for this study was approved on the 23rd of August 2022 by the Ethics Committee of the Ribeirão Preto Dental School at the University of São Paulo - CEUA (protocol # 2022.1.534.58.0). Brazilian guidelines for animal experiments were adhered to. The study was conducted in accordance with ARRIVE guidelines.

2.2. Study Design

A total of 48 specially manufactured titanium implants with a novel design of different decompressive cervical blade profiles were used for this research. The implants received conventional surface treatment recommended by the company, involving a double acid etching process, and have a surface roughness of Ra = 1.3 μm (Leader Medica – Medical Technology – Pádua, Italy). They had a diameter of 3.75mm and a height of 10mm, divided into three groups based on differences in the size of the decompressive cervical blades:

Control Group (CG-0): Neutral blade (0.0 mm) / no radial difference.

Test Group 1 (TG-50): Blades with a radial difference of +0.05 mm, resulting in mild bone decompression.

Test Group 2 (TG-200): Blades with a radial difference of +0.2 mm, resulting in greater bone decompression.

Two implants were installed in the medial segment of the tibia bilaterally, with distribution and randomization into the three different experimental groups, in the metaphyseal and diaphyseal regions of each animal, following the methodology described by Caneva et al., 2014 [29]. The osteotomies were performed uniformly in all experimental sites, following the sequence of drills

 doi:10.20944/preprints202407.0788.v1

recommended by the manufacturer: Starter, 2.40 mm; 2.80 mm; 3.2 mm; 3.4 mm; 3.65 mm; 3.75 mm (Leader Medica – Medical Technology – Pádua, Italy).

2.3. Experimental animals and sample size

An experimental, prospective, and randomized study was conducted with test and control implants in the same animal, eliminating interference between individuals within the same group and allowing for the use of a reduced number of animals with sample representativeness.

A previous study in dogs evaluated the influence of different torques (70 Ncm vs. 30 Ncm) on implant osseointegration, in which higher torque means more compression on the recipient bone (23, Kotsu). A mean difference in bone-to-implant contact of 9.4% was observed in favor of the lower torque. With a calculated effect size 2.57, applying an α=0.05, a power of 0.9, a two-tails evaluation resulted in a sample size of 5 pairs of animals to reject the null hypothesis that the difference is zero (G*Power 3.1.9.4) [29,30]. However, considering multiple comparison corrections and possible complications and death of animals, the number was increased to 12 animals. Hence, twelve adult female New Zealand White rabbits weighing 3.5–4.0 kg were used.

2.4. Randomization and allocation concealment

Randomization of the test and control groups were conducted electronically by an author not involved in the selection and handling of animals and/or surgical procedures (S.P.X.). The treatment allocations were ensured in sealed opaque envelopes opened immediately before tibia drilling.

2.5. Implants characteristics

The implants used (CortyBlade® Leader Medica s.r.l., via Giacinto Andrea Longhin 11, 35129 Padova, PD, Italy) were 3.75 mm of diameter and 8.5 mm of length with a tapered one-piece conformation with double acid-etched surface. The transmucosal collar was 1.8 mm high, with a convergent conformation. The CortyBlade implants were equipped with blades in the coronal aspect aiming to create bone decompression in the cortical layer. Implants with four different blade diameters were used. The difference in diameter of the blades in relation to the neck of the implant was as follows: 0 μm (control site; CG-0), +50 μm (test site; TG-50), or +200 μm (test site; TG-200) (Figure 1).

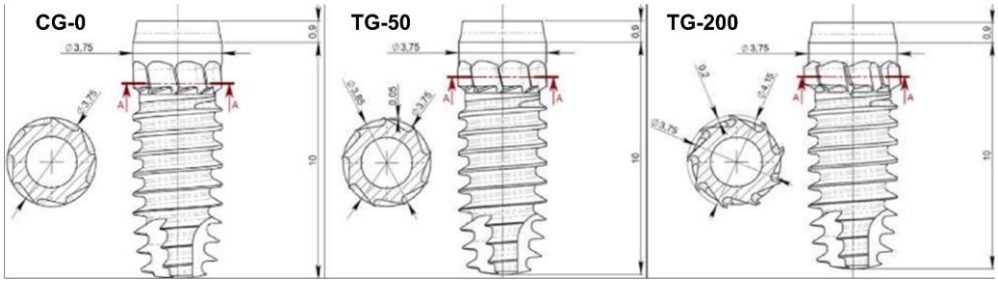

Figure 1. Technical design of osseointegrated implants (CortyBlade® Leader Medica, Italy). GC-0 – Implant with neutral blade (without radial difference). GT-50 – Implant with decompressive blades with a radial difference of +50 μm. GT-200 – Implant with decompressive blades with a radial difference of +200 μm.

2.6. Anesthesia and Medications Procedures

Sedation was performed with Acepromazine 1.0 mg/kg (Acepran®, Vetnil, Louveira, São Paulo, Brazil) administered intramuscularly (IM). Subsequently, anesthesia was induced with Xylazine 3.0 mg/kg (Dopaser®, Hertape Calier, Juatuba, Minas Gerais, Brazil) and Ketamine Hydrochloride 50 mg/kg (Ketamin Agener, União Química Farmacêutica Nacional S/A, Embu-Guaçu, São Paulo, Brazil) IM. Local anesthesia was performed using 2% Mepivacaine with 1:100,000 Epinephrine (Mepiadre, Nova DFL, Rio de Janeiro, Brazil) in the experimental regions. In the preoperative period, animals

 doi:10.20944/preprints202407.0788.v1

received a prophylactic dose of Oxytetracycline 20 mg/kg IM (Biovet, Vargem Grande Paulista, São Paulo, Brazil), 0.2% Meloxicam (Framavet, 1.0 mg/kg, s.c.; União Química Farmacêutica Nacional S/A., Embu-Guaçu, São Paulo, Brazil), and Tramadol Hydrochloride 5.0 mg/kg s.c. (Halexlstar; Goiânia, Goiás, Brazil). Anti-inflammatory (Meloxicam 0.2%, Flamavet, 0.5 mg/kg, s.c.; União Química Farmacêutica Nacional S/A., Embu-Guaçu, São Paulo, Brazil) and analgesic medications (Tramadol Hydrochloride, 5.0 mg/kg, s.c., Halex Istar, Goiânia, Goiás, Brazil) were administered once daily for the first two postoperative days.

2.7. Surgical Procedure

The areas to be operated were shaved, and antiseptic preparation was performed by topically applying 1% Povidone-Iodine solution (Riodeine Tincture, Rioquímica, São José do Rio Preto, São Paulo, Brazil). Local anesthesia was administered as described above. All surgeries were performed by a single experienced and trained operator.

A linear incision of 2.5 to 3 cm was made on the skin in the medial segment of the tibia bilaterally, and the skin and periosteum were retracted. Two experimental sites were identified in each tibia, the metaphyseal and diaphyseal regions, approximately 10 mm apart (Figure 2).

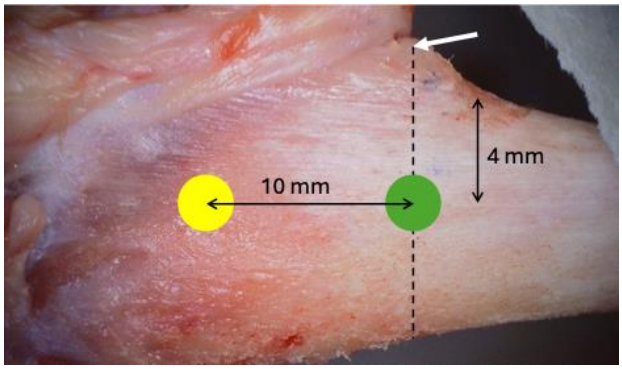

Figure 2. Anatomical specimen demonstrating reference regions for selecting experimental sites. The white arrow indicates the tibial tuberosity that serves as a reference for the tibial diaphysis region. The green circle represents the selection of the experimental site in the tibial diaphysis. The yellow circle is 10 mm away from the green circle, indicating the experimental site in the tibial metaphysis.

Identical osteotomies using the predetermined drill sequence (Figure 3A). At this point, the treatment allocation was revealed to the surgeon. Implants with modified blade designs were inserted so that their prosthetic platform was positioned at about the bone level (Figure 3B), and their apices were anchored in the inner cortex of the tibia, following the protocol described by Caneva et al., 2014. Torque insertion measurements at the final position was recorded using a wrench included in the surgical kit. Cover screws were placed (Figure 3C) and sutures were provided in layers using 4-0 Nylon (Ethicon®, Johnson & Johnson®, São José dos Campos, São Paulo, Brazil), and a bandage strip was placed over the wound, remaining in place for three days of the postoperative period.

 doi:10.20944/preprints202407.0788.v1

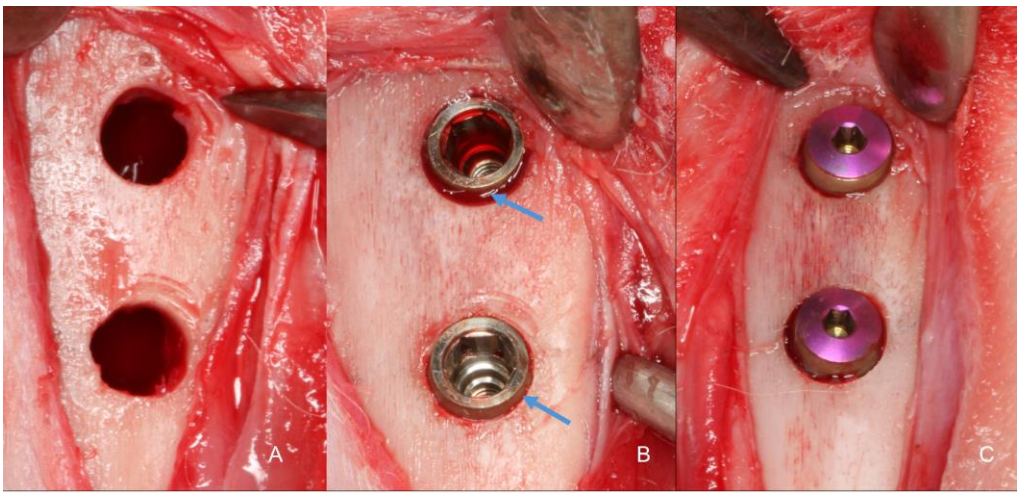

Figure 3. Intraoperative images. A: Surgical site prepared for implant installation (below the diaphysis region and above the metaphysis region). B: implants installed in their final position. The blue arrow shows the region decompressed by the Cortyblade. C: cover screws installed on the implants.

2.8. Animal Maintenance

For a preoperative adaptation period of two weeks and throughout the postoperative period the rabbits were kept in individual cages without specific bedding, but with a small plastic support for resting their paws (1 animal/6000cm^2). The room where they were housed had a Split air conditioner (21°C) without humidity control, and 27 to 34 air changes per hour were performed. There was an automatic lighting control every 12/12 hours, and ad libitum filtered food and water were provided. Sanitary barriers, including an autoclave, sanitary facilities/locker rooms, and insect control screens, were available. After the surgical procedure, rabbits were placed in specific cages for motion control for two days, and then they returned to their cages, being observed daily for signs of pain and/or infection at the surgical wound site until the time of euthanasia.

2.9. Euthanasia

After 10 weeks of the postoperative period, euthanasia wsa performed (n = 12). Firstly, sedation was administered with Acepromazine 1.0 mg/kg (Acepran®, Vetnil, Louveira, São Paulo, Brazil), followed by anesthesia through the combination of Xylazine 3.0 mg/kg (Dopaser®, Hertape Calier, Juatuba, Minas Gerais, Brazil) and Ketamine Hydrochloride 50 mg/kg (Ketamin Agener, União Química Farmacêutica Nacional S/A., Embu-Guaçu, São Paulo, Brazil), administered via IM. Subsequently, the animals were individually placed in a CO^2 chamber with controlled flow of 7 L/min at a rate of 20% of the total volume. This flow was maintained for at least 1 minute after confirming clinical death of the animal, checking for signs of respiratory arrest, mucosal cyanosis, and absence of a pulse. Biopsies of the operated sites were collected and immediately immersed in 10% paraformaldehyde solution.

2.10. Histological Processing

The specimens were dehydrated in a sequence of alcohol solutions and then embedded in resin (LR WhiteTM HardGrid, London Resin Co Ltd, Berkshire, United Kingdom). After polymerization, each block was cut in a coronal plane guided by the center of the implant. Two sections of approximately 100-150 µm were prepared using a precision cutting device (Exakt, Apparatebau, Norderstedt, Germany) and sanded until obtaining approximately 50-60 µm thick were obtained. Histological sections were stained using Toluidine Blue, Stevenel's Blue, and Alizarin Red.

2.11. Histological Evaluation

All measurements were made by a single examiner (V.B.F.). Before starting the histological measurements, a specialist (S.P.X.) calibrated the examiner responsible for the analyzes until

 doi:10.20944/preprints202407.0788.v1

obtaining an inter-examiner kappa > 0.9. Images were taken at about x100 magnification. Histological evaluations were conducted in three implant regions (coronal, marrow, and apical; Figure 4A) using Image J software version 1.54d (NIH, Bethesda, MD, USA). In the coronal region, bone-to-implant contact was measured in two different regions, i.e., the collar region (decompressive zone) and the blade region (Figure 4B).

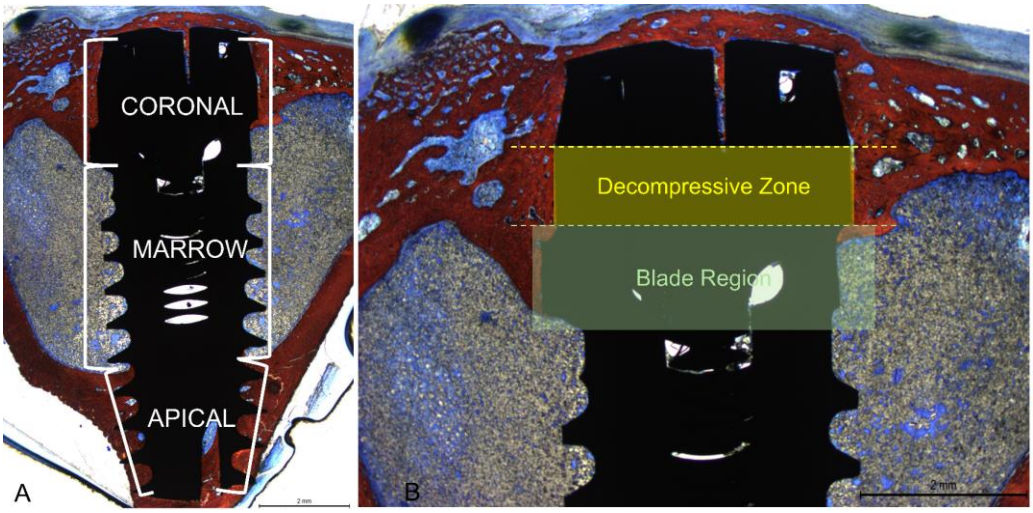

Figure 4. A: Photomicrograph demonstrating the total length of the implant and the three regions evaluated: coronal, marrow and apical. B: Photomicrograph under 16x magnification of the implant coronal region of. In yellow, the decompressive zone in the cervical collar is represented. In green, the region of the cortical blades.

Mean values were obtained to express the BIC% in the coronal region. New bone was also evaluated in the apical region between the coronal and apical extensions of integration. Osseointegration was also evaluated in the marrow compartment from the base of the blades and the internal limits of the apical cortical layer. Newly formed bone and soft tissues (medullary spaces and osteons) were evaluated.

2.12. Statistical Analysis

Four implants were inserted into each animal tibia, with one group out of three randomly receiving two implants per animal. A mean value of these two implants was calculated so that each group was represented once for each animal (n=12). The primary variable was the percentage of bone in contact with the implant surface in the decompressive region, while osseointegration extension in the coronal region and BIC% in other regions were considered secondary variables. Data normality was evaluated using the Shapiro-Wilk test. Depending on the results, either an ANOVA or a Friedman test was applied for group comparisons. Differences were analyzed using a paired t-test or a Wilcoxon test. Data were stored in an Excel file (Microsoft® Excel® V. 2404) for descriptive statistics. Statistical analyses were conducted using Prism Software (GraphPad Software, LLC, San Diego, CA, USA), with an alpha level of 5%.

3. Results

3.1. Clinical outcomes

All animals healed uneventfully, and all implants were available for histological processing. No implants were lost resulting in n=12.

3.2. Descriptive histological evaluation

All histological slides were available for analysis. All implants presented optimal osseointegration without marginal bone loss (Figure 5 A-C).

 doi:10.20944/preprints202407.0788.v1

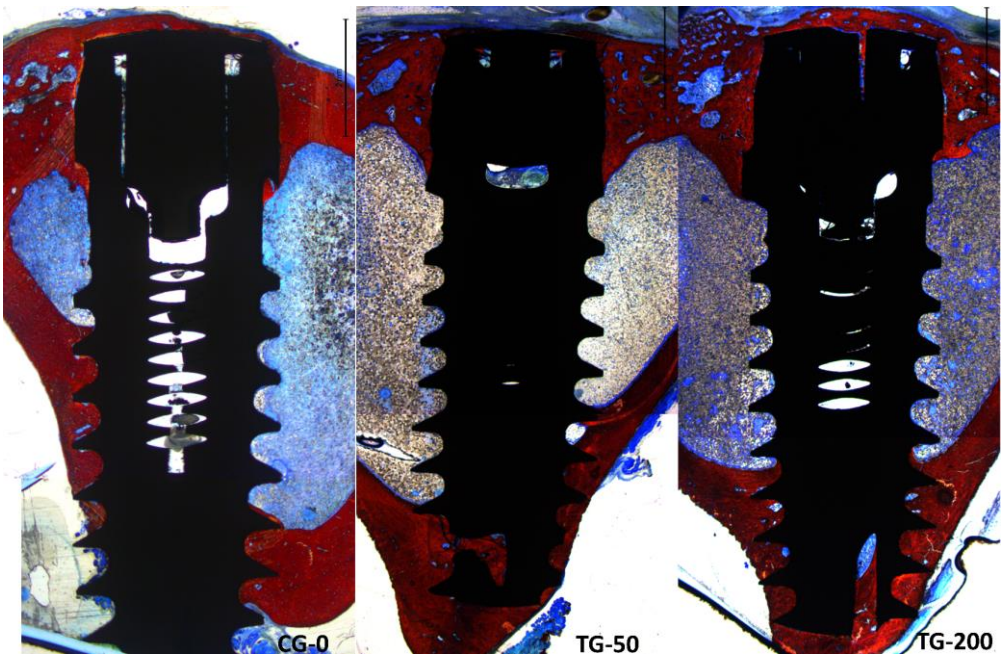

Figure 5. Photomicrograph of ground sections showing the healing at the 3 different implants. CG-O represents the implant with the blades without radial difference. TG-50 represents the implant with blades with a radial difference of +50 μm. TG-200 represents the implant with blades with a radial difference of +200 μm.

Instead, all implants exhibited new bone formation in the coronal region. Complete closure was observed in the CG-0 group (Figure 6A), as well as in the TG-50 (Figure 6B) and TG-200 (Figure 6C) groups, despite the presence of marginal gaps without primary bone contact at installation.

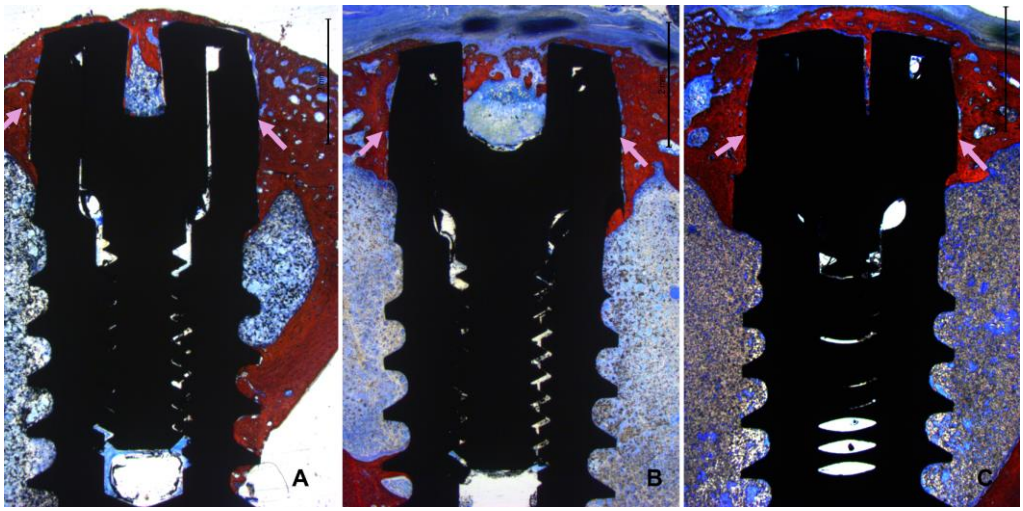

Figure 6. Photomicrograph of ground sections showing the healing at the 3 different implants. A: CG-0; B: TG -50; C: TG-200. The pink arrows demonstrate the decompressed region completely filled with new bone.

In the apical region, several implants breached the cortical layer (Figure 7 A,B). Nevertheless, new bone formation in this region completely closed the osteotomy, effectively isolating the internal environment of the tibia from the external.

 doi:10.20944/preprints202407.0788.v1

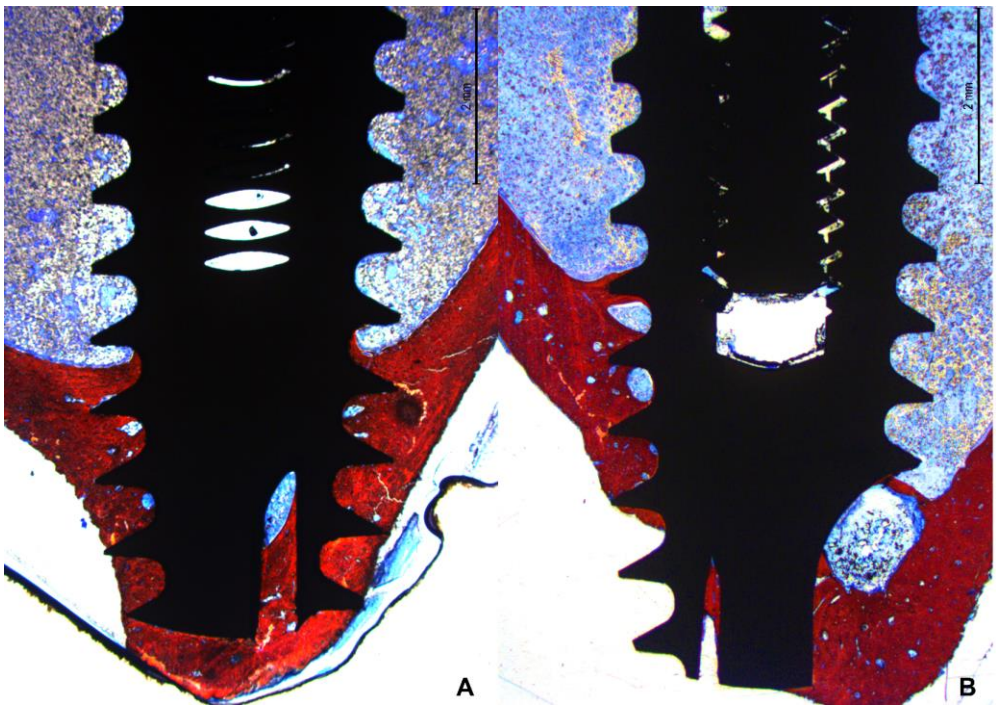

Figure 7. Photomicrograph under 16x magnification of the implant apical region. A: Implant apical area with apex perfectly inserted at the cortical layer. B: Apical region of the implant surpassing the cortical layer, however complete closure of the region with new bone is observed.

The newly formed bone predominantly accumulated near the two cortical layers, spreading toward the marrow region, which generally lacked new bone between the coronal and apical regions. Only when the implant was close to the lateral cortical walls did new bone extend into the marrow region between the cortex and the implant surface (Figure 8 A,B).

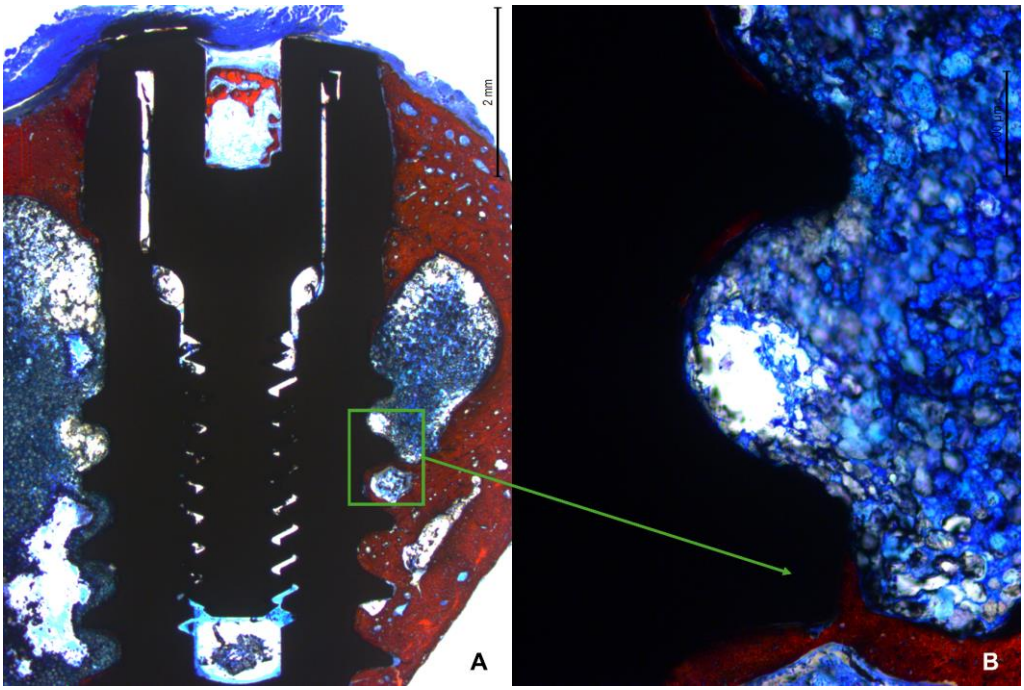

Figure 8. A: Photomicrograph under 16x magnification. B: Photomicrograph under 100X magnification. The region highlighted in green demonstrates bone formation in the medullary region starting from the lateral cortex.

 doi:10.20944/preprints202407.0788.v1

No significant differences in the healing process were observed between implants placed in the diaphysis and those near the metaphysis.

3.3. Histomorphometric assessments

In the decompressive region (collar), similar amounts of newly formed bone were observed in all groups, the mean values ranging between 60.6-63.6% (Table 1). In the blade zone, statistically significant higher proportions of new bone were found in the CG-0 group (53.4%) compared to TG-50 (33.6%) and TG-200 (34.4%). Merging the data between decompressive and blade zone no statistically significant differences were obtained.

Table 1. Bone to implant contact percentage in the various region analyzed. Mean values ± standard deviation. * = p<0.05.

Groups	Coronal	Decompressive	Blades	Marrow	Apical	Total
CG-0	57.0 ±15.0	60.6 ±16.5	53.4 ±23.3*	9.4 ±4.4	71.8 ±12.8	38.6 ±7.3
TG-50	48.6 ±10.3	63.6 ±18.0	33.6 ±14.7*	10.0 ±6.2	77.8 ±11.4	40.7 ±6.5
TG-200	47.8 ±12.5	61.2 ±16.2	34.4 ±15.5*	10.4 ±11.5	78.8 ±7.2	42.0 ±8.3

The mean value of the cortical layer was 1.31 ±0.29 mm. The apical extension of osteointegration from the implant shoulder considering all implants was 2.68 ±0.33 mm for CG-0, 2.41 ±0.27 mm for TG-50, and 2.32 ±0.38 mm for the TG-200.

High fractions of new bone were found also in the apical region in all implants, the mean values ranging between 71.8-78.8%. Higher percentages were found at the implant with marginal defects.

In the marrow space, very low percentages of new bone were found in all groups, the mean value ranging between 9.4% – 10.4%. The total percentage of new bone on the implant surface was similar in all groups, the mean values ranging between 38.6-42.0%.

4. Discussion

The decompression zone exhibited a similar amount of osseointegration across all groups, even those with marginal defects. However, in the blade region, the CG-0 group demonstrated higher osseointegration compared to the test groups. Additionally, a high percentage of osseointegration was observed in the apical region across all groups.

The use of blades in the cortical region was meant to reduce the compression at the cortical layer. The compression of this region might create strain in the peri-implant bone, negatively impacting osteocyte survival. This high strain restricts blood flow and results in microdamage to the bone, leading to osteocyte necrosis, significant bone remodeling, and limited new bone formation [33]. Blades of three different dimensions were utilized to widen the coronal aspect of the osteotomies in the decompression region, matching the diameter of the collar or leaving a residual gap of either 50 μm or 200 μm after implant installation. The cortical regions in all specimens, including those with an initial gap, were completely filled with newly formed bone. The implants were positioned so that the prosthetic platform was close to the cortical layer, with the intention of having the blades pass beyond the lower limit of the cortical layer to prevent contact between the two structures. Specifically, the coronal level of the blade was fabricated 1.9 mm from the prosthetic platform, while the mean width of the cortical layer was 1.3 mm. Despite the absence of primary contact between the collar and the cortical layer, it can be assumed that the gap between the collar and the osteotomy in the two test groups was filled with new bone through distance or contact osteogenesis [34,35]. This result is in agreement with a study in which a chamber 0.4 mm in depth was created around implants with either a moderate rough or a turned surface [26,36]. New bone was found on the implant surface within the chamber already after 1 weeks. A higher percentage of new bone formation was observed on the rough surface compared to the turned surface. In another similar experiment, chamber deeper that 0.5 mm were prepared around implants [27]. Again, new bone was found on the implant surface after 2 weeks of healing. Although the distances in the aforementioned studies were significantly greater than those used in the present study, a key difference is that no contact between the bone and implant

 doi:10.20944/preprints202407.0788.v1

surface was permitted in the present study, whereas in the chamber studies, the threads near the chambers were in close contact with the bone walls of the osteotomy. New bone formation could have occurred from the osteotomy and spread onto the implant surface due to the osteoconductive properties of the implant surface. Indeed, in other experiments where marginal circumferential defects of 0.5-1.25 mm were created around implants, it was demonstrated that new bone formation occurred from the lateral walls [37,38], reaching a distance of 0.4 mm from the implant surface within 20 days, regardless of the initial size of the gap [39]. The remaining 0.4 mm defect was subsequently closed over time by new bone forming on the implant surface from the bottom of the defect where the implant was in close contact with the bone. This process was facilitated by the osteoconductive properties of the implant surface [40]. In contrast, other experimental studies [41,42] observed minimal integration when no contact was allowed between the bone walls of the osteotomy and the body of the implant, especially in marginal defects ranging from 0.7-1.20 mm or 0.35-0.85 mm. The formation of woven bone was halted at around 0.4-0.5 mm from the implant surface, preventing direct contact with the implant surface. Additionally, the use of deproteinized bovine bone mineral did not promote osseointegration in these studies [43]. However, in the present study, complete closure of the gap around the collar of the implant was achieved, even in the absence of primary bone contact. This suggests that new bone formation, either through distance or contact osteogenesis, occurred and integrated onto the implant surface.

Indeed, a notable distinction in the present study compared to the previously mentioned ones is the smaller dimension of the gaps, which were less than 0.4 mm (50 μm and 200 μm). This short "jumping distance," as described by Botticelli [38], may facilitate bone formation on the implant surface through contact or distance osteogenesis [34,35]. Another unique aspect is the formation of bone chips by the blades, which fill the gap around the implant collar, as observed in a dog experiment [44]. It has been demonstrated that bone debris can serve as bridges for the formation of osteoid tissue and newly formed bone, as supported by studies by human [45,46] and animal studies [47]. These factors likely contributed to the observed osseointegration and closure of the gaps around the implant collar in the present study.

The greater extension of osseointegration in an apical direction observed in the control group compared to the test groups, along with the higher percentage of bone-to-implant contact (BIC%), suggests potentially favorable outcomes with the CG-0 group. Additionally, the similar BIC% in the decompression zone further supports this notion. It is worth noting that implants with blades have previously shown success in experiments conducted in dogs [44]. Interestingly, similar levels of marginal resorption were noted across different blade conformations, with a trend towards lower resorption observed for the 50 μm blade. This collective evidence underscores the potential efficacy and versatility of implants equipped with blades in promoting osseointegration and minimizing marginal resorption.

The present study demonstrated that all implants were successfully integrated in both cortical layers, with higher bone-to-implant contact percentages (BIC%) observed in the apical regions compared to the coronal regions. This apical integration suggests optimal initial implant stability, even in the absence of contact in the coronal region, in both the TG-50 and TG-200 groups. This finding aligns with observations from other experiments [29–32,48] and provides further support to the outcomes reported in various clinical studies where bicortical installation was employed [49–53].

The primary limitations of the present study pertain to the phylogenetic differences between rabbits and humans, as well as the distinct anatomical and physiological characteristics of the tibia compared to the alveolar bone crest. Consequently, any inferences should be confined to the histological findings and not directly extrapolated to clinical settings. Nonetheless, the data generated from this study provide a valuable foundation for subsequent clinical research aimed at confirming these findings.

Conclusions

The use of a blade attached to the implant body enabled precise preparation of the cortical layer, allowing for controlled decompression in the targeted area. This technique resulted in optimal

osseointegration with no loss of marginal bone, and complete restoration of marginal gaps ranging from 0 μm to 200 μm.

Author Contributions: Conceptualisation, V.F.B., M.F and D.B.; methodology, V.F.B., E.R.S., D.B. and S.P.X.; validation, E.P.G. and L.G.A.; formal analysis, V.F.B. and D.B..; investigation, V.F.B., M.F., E.P.G. and L.G.A.; resources, M.F. and D.B.; data curation, V.F.B. and D.B.; writing-original draft preparation, V.F.B. and D.B.; writing-review and editing, V.F.B., D.B., E.R.S. and S.P.X.; visualisation, E.P.G. and L.G.A.; supervision, D.B. and S.P.X; project administration, S.P.X.; funding acquisition, M.F. and D.B. All authors have read and agreed to the published version of the manuscript.".

Funding: This research was funded by ARDEC Academy srl and Leader Medica s.r.l.

Institutional Review Board Statement: Not applicable.

Informed Consent Statement: Not applicable.

Data Availability Statement: Data are available on reasonable request.

Conflicts of Interest: all authors declaire no conflit of interest.

Acknowledgements: The authors thanks Sebastiao Bianco, Faculty of Odontology, Ribeirão Preto (USP), Brazil for the histological processing and Marco Guzzo, Brenta Engineering, Noventa Padovana, PD, Italy for the technical support in implant design. The implants were provided by Leader Medica s.r.l. free of charge.

References

1. Gehrke SA, Prados-Frutos JC, Prados-Privado M, Calvo-Guirado JL, Aramburú Júnior J, Pérez-Díaz L, Mazón P, Aragoneses JM, De Aza PN. Biomechanical and Histological Analysis of Titanium (Machined and Treated Surface) Versus Zirconia Implant Materials: An In Vivo Animal Study. Materials (Basel). 2019 Mar 14;12(6):856. doi: 10.3390/ma12060856. PMID: 30875729; PMCID: PMC6471506.
2. Hanawa T. Titanium-Tissue Interface Reaction and Its Control With Surface Treatment. Front Bioeng Biotechnol. 2019 Jul 17;7:170. doi: 10.3389/fbioe.2019.00170. PMID: 31380361; PMCID: PMC6650641
3. Elias CN, Fernandes DJ, Resende CR, Roestel J. Mechanical properties, surface morphology and stability of a modified commercially pure high strength titanium alloy for dental implants. Dent Mater. 2015 Feb;31(2):e1-e13. doi: 10.1016/j.dental.2014.10.002. Epub 2014 Nov 13. PMID: 25458351.
4. Alghamdi HS. Methods to Improve Osseointegration of Dental Implants in Low Quality (Type-IV) Bone: An Overview. J Funct Biomater. 2018 Jan 13;9(1):7. doi: 10.3390/jfb9010007. PMID: 29342830; PMCID: PMC5872093.
5. Sartoretto SC, Calasans-Maia JA, Costa YOD, Louro RS, Granjeiro JM, CalasansMaia MD. Accelerated Healing Period with Hydrophilic Implant Placed in Sheep Tibia. Braz Dent J. 2017 Sep-Oct;28(5):559-565. doi: 10.1590/0103-6440201601559. PMID: 29215679.
6. Gehrke SA, Dedavid BA, Aramburú JS Júnior, Pérez-Díaz L, Calvo Guirado JL, Canales PM, De Aza PN. Effect of Different Morphology of Titanium Surface on the Bone Healing in Defects Filled Only with Blood Clot: A New Animal Study Design. Biomed Res Int. 2018 Aug 8;2018:4265474. doi: 10.1155/2018/4265474. PMID: 30175131; PMCID: PMC6106843.
7. Lukaszewska-Kuska M, Wirstlein P, Majchrowski R, Dorocka-Bobkowska B. Osteoblastic cell behaviour on modified titanium surfaces. Micron. 2018 Feb;105:55- 63. doi: 10.1016/j.micron.2017.11.010. Epub 2017 Nov 22. PMID: 29179009.
8. Pellegrini G, Francetti L, Barbaro B, Del Fabbro M. Novel surfaces and osseointegration in implant dentistry. J Investig Clin Dent. 2018 Nov;9(4):e12349. doi: 10.1111/jicd.12349. Epub 2018 Jul 4. PMID: 29971928.
9. Coelho PG, Granato R, Marin C, Teixeira HS, Suzuki M, Valverde GB, Janal MN, Lilin T, Bonfante EA. The effect of different implant macrogeometries and surface treatment in early biomechanical fixation: an experimental study in dogs. J Mech Behav Biomed Mater. 2011 Nov;4(8):1974-81. doi: 10.1016/j.jmbbm.2011.06.016. Epub 2011 Jul 3. PMID: 22098896.
10. Gehrke SA, Eliers Treichel TL, Pérez-Díaz L, Calvo-Guirado JL, Aramburú Júnior J, Mazón P, de Aza PN. Impact of Different Titanium Implant Thread Designs on Bone Healing: A Biomechanical and Histometric Study with an Animal Model. J Clin Med. 2019 May 31;8(6):777. doi: 10.3390/jcm8060777. PMID: 31159286; PMCID: PMC6616501.
11. Negri B, Calvo-Guirado JL, Maté Sánchez de Val JE, Delgado Ruiz RA, Ramírez Fernández MP, Gómez Moreno G, Aguilar Salvatierra A, Guardia J, Muñoz Guzón F. Biomechanical and bone histomorphological evaluation of two surfaces on tapered and cylindrical root form implants: an experimental study in dogs.

Clin Implant Dent Relat Res. 2013 Dec;15(6):799-808. doi: 10.1111/j.1708-8208.2011.00431.x. Epub 2012 Jan 11. PMID: 22236466.

12. Trisi P, Perfetti G, Baldoni E, Berardi D, Colagiovanni M, Scogna G. Implant micromotion is related to peak insertion torque and bone density. Clin Oral Implants 19 Res. 2009 May;20(5):467-71. doi: 10.1111/j.1600-0501.2008.01679.x. PMID: 19522976.
13. Martinez H, Davarpanah M, Missika P, Celletti R, Lazzara R. Optimal implant stabilization in low density bone. Clin Oral Implants Res. 2001 Oct;12(5):423-32. doi: 10.1034/j.1600-0501.2001.120501.x. PMID: 11564101.
14. Friberg B, Ekestubbe A, Mellström D, Sennerby L. Brånemark implants and osteoporosis: a clinical exploratory study. Clin Implant Dent Relat Res. 2001;3(1):50- 6. doi: 10.1111/j.1708-8208.2001.tb00128.x. PMID: 11441543.
15. Eskan, M.A., Uzel, G. & Yilmaz, S. A fixed reconstruction of fully edentulous patients with immediate function using an apically tapered implant design: a retrospective clinical study. Int J Implant Dent 6, 77 (2020). https://doi.org/10.1186/s40729-020-00271-1
16. Gehrke SA, Júnior JA, Treichel TLE, do Prado TD, Dedavid BA, de Aza PN. Effects of insertion torque values on the marginal bone loss of dental implants installed in sheep mandibles. Sci Rep. 2022 Jan 11;12(1):538. doi: 10.1038/s41598.021.04313.5. PMID: 35017552; PMCID: PMC8752839.
17. Trisi P, Todisco M, Consolo U, Travaglini D. High versus low implant insertion torque: a histologic, histomorphometric, and biomechanical study in the sheep mandible. Int J Oral Maxillofac Implants. 2011 Jul-Aug;26(4):837-49. PMID: 21841994.
18. Scarano A, Piattelli A, Assenza B, Sollazzo V, Lucchese A, Carinci F. Assessment of pain associated with insertion torque of dental implants. A prospective, randomizedcontrolled study. Int J Immunopathol Pharmacol. 2011 Apr-Jun;24(2 Suppl):65-9. doi: 10.1177/03946320110240S212. PMID: 21781448.
19. Norton MR. The Influence of Low Insertion Torque on Primary Stability, Implant Survival, and Maintenance of Marginal Bone Levels: A Closed-Cohort Prospective Study. Int J Oral Maxillofac Implants. 2017 Jul/Aug;32(4):849-857. doi: 10.11607/jomi.5889. PMID: 28708918.
20. Aldahlawi S, Demeter A, Irinakis T. The effect of implant placement torque on crestal bone remodeling after 1 year of loading. Clin Cosmet Investig Dent. 2018 Oct 9;10:203-209. doi: 10.2147/CCIDE.S174895. PMID: 30349398; PMCID: PMC6183656.
21. Campos FE, Jimbo R, Bonfante EA, Barbosa DZ, Oliveira MT, Janal MN, Coelho PG. Are insertion torque and early osseointegration proportional? A histologic evaluation. Clin Oral Implants Res. 2015 Nov;26(11):1256-60. doi: 10.1111/clr.12448. Epub 2014 Jul 4. PMID: 24995491.
22. Rea M, Lang NP, Ricci S, Mintrone F, González González G, Botticelli D. Healing of implants installed in over- or under-prepared sites--an experimental study in dogs. Clin Oral Implants Res. 2015 Apr;26(4):442-446. doi: 10.1111/clr.12390. Epub 2014 Mar 31. PMID: 24684411.
23. Kotsu M, Urbizo Velez J, Bengazi F, Tumedei M, Fujiwara S, Kato S, Botticelli D. Healing at implants installed from ~ 70- to < 10-Ncm insertion torques: an experimental study in dogs. Oral Maxillofac Surg. 2021 Mar;25(1):55-64. doi: 10.1007/s10006-020-00890-3. Epub 2020 Jul 29. PMID: 32725574.
24. Jimbo R, Tovar N, Anchieta RB, Machado LS, Marin C, Teixeira HS, Coelho PG. The combined effects of undersized drilling and implant macrogeometry on bone healing around dental implants: an experimental study. Int J Oral Maxillofac Surg. 2014 Oct;43(10):1269-75. doi: 10.1016/j.ijom.2014.03.017. Epub 2014 May 1. PMID: 24794761.
25. Berardini M, Trisi P, Sinjari B, Rutjes AW, Caputi S. The Effects of High Insertion Torque Versus Low Insertion Torque on Marginal Bone Resorption and Implant Failure Rates: A Systematic Review With Meta-Analyses. Implant Dent. 2016 Aug;25(4):532-40. doi: 10.1097/ID.0000000000000422. PMID: 27129002.
26. Abrahamsson I, Berglundh T, Linder E, Lang NP, Lindhe J. Early bone formation adjacent to rough and turned endosseous implant surfaces. An experimental study in the dog. Clin Oral Implants Res. 2004 Aug;15(4):381-92. doi: 10.1111/j.1600-0501.2004.01082.x. PMID: 15248872.
27. Buser D, Broggini N, Wieland M, Schenk RK, Denzer AJ, Cochran DL, Hoffmann B, Lussi A, Steinemann SG. Enhanced bone apposition to a chemically modified SLA titanium surface. J Dent Res. 2004 Jul;83(7):529-33. doi: 10.1177/154405910408300704. PMID: 15218041.
28. Stübinger S, Dard M. The rabbit as experimental model for research in implant dentistry and related tissue regeneration. J Invest Surg. 2013 Oct;26(5):266-82. doi: 10.3109/08941939.2013.778922. Epub 2013 Apr 25. PMID: 23617292.
29. Caneva M, Lang NP, Calvo Guirado JL, Spriano S, Iezzi G, Botticelli D. Bone healing at bicortically installed implants with different surface configurations. An experimental study in rabbits. Clin Oral Implants Res. 2015;26:293-9
30. Soto-Peñaloza D, Caneva M, Viña-Almunia J, Martín-de-Llano JJ, PeñarrochaOltra D, Peñarrocha-Diago M. Bone-Healing Pattern on the Surface of Titanium Implants at Cortical and Marrow Compartments in Two Topographic Sites: an Experimental Study in Rabbits. Materials (Basel). 2018 Dec 27;12(1):85. doi: 10.3390/ma12010085. PMID: 30591652; PMCID: PMC6337604.

31. Soto-Peñaloza D, Caneva M, Viña-Almunia J, Martin-de-Llano JJ, García-Mira B, Peñarrocha-Oltra D, Botticelli D, Peñarrocha-Diago M. Effect on osseointegration of two implant macro-designs:A histomorphometric analysis of bicortically installed implants in different topographic sites of rabbit's tibiae. Med Oral Patol Oral Cir Bucal. 2019 Jul 1;24(4):e502-e510. doi: 10.4317/medoral.22825. PMID: 31232382; PMCID: PMC6667005.
32. Feletto L, Bengazi F, Urbizo Velez JJ, Ferri M, Favero R, Botticelli D. Bone healing at collagenated bicortically installed implants: an experimental study in rabbits. Oral Maxillofac Surg. 2020 Dec;24(4):501-507. doi: 10.1007/s10006-020-00882-3. Epub 2020 Jul 11. PMID: 32653997
33. Cha JY, Pereira MD, Smith AA, Houschyar KS, Yin X, Mouraret S, Brunski JB, Helms JA. Multiscale analyses of the bone-implant interface. J Dent Res. 2015 Mar;94(3):482-90. doi: 10.1177/0022034514566029. Epub 2015 Jan 27. PMID: 25628271; PMCID: PMC4814020.
34. Davies, J.E. (1998) Mechanisms of endosseous integration. The International Journal of Prosthodontics 11: 391–401.
35. Davies, J.E. (2003) Understanding peri-implant endosseous healing. Journal of Dental Education 67: 932–49.
36. Berglundh T, Abrahamsson I, Lang NP, Lindhe J. De novo alveolar bone formation adjacent to endosseous implants. Clin Oral Implants Res. 2003 Jun;14(3):251-62. doi: 10.1034/j.1600-0501.2003.00972.x. PMID: 12755774.
37. Botticelli D, Berglundh T, Buser D, Lindhe J. Appositional bone formation in marginal defects at implants. Clin Oral Implants Res. 2003 Feb;14(1):1-9. doi: 10.1034/j.1600-0501.2003.140101.x. PMID: 12562359.
38. Botticelli D, Berglundh T, Buser D, Lindhe J. The jumping distance revisited: An experimental study in the dog. Clin Oral Implants Res. 2003 Feb;14(1):35-42. doi: 10.1034/j.1600-0501.2003.140105.x. PMID: 12562363.
39. Rossi F, Botticelli D, Pantani F, Pereira FP, Salata LA, Lang NP. Bone healing pattern in surgically created circumferential defects around submerged implants: an experimental study in dog. Clin Oral Implants Res. 2012 Jan;23(1):41-8. doi: 10.1111/j.1600-0501.2011.02170.x. Epub 2011 Mar 28. PMID: 21443594.
40. Botticelli D, Berglundh T, Persson LG, Lindhe J. Bone regeneration at implants with turned or rough surfaces in self-contained defects. An experimental study in the dog. J Clin Periodontol. 2005 May;32(5):448-55. doi: 10.1111/j.1600-051X.2005.00693.x. PMID: 15842258.
41. Sivolella S, Bressan E, Salata LA, Urrutia ZA, Lang NP, Botticelli D. Osteogenesis at implants without primary bone contact - an experimental study in dogs. Clin Oral Implants Res. 2012 May;23(5):542-9. doi: 10.1111/j.1600-0501.2012.02423.x. Epub 2012 Feb 15. PMID: 22335282.
42. Carlsson L, Röstlund T, Albrektsson B, Albrektsson T. Implant fixation improved by close fit. Cylindrical implant-bone interface studied in rabbits. Acta Orthop Scand. 1988 Jun;59(3):272-5. doi: 10.3109/17453678809149361. PMID: 3381657.
43. Sivolella S, Bressan E, Salata LA, Quiñones ME, Lang NP, Botticelli D. Deproteinized bovine bone mineral particles and osseointegration of implants without primary bone contact: an experimental study in dogs. Clin Oral Implants Res. 2014 Mar;25(3):296-303. doi: 10.1111/clr.12154. Epub 2013 Apr 8. PMID: 23560606.
44. Kanayama M, Ferri M, Guzon FMM, Asano A, Alccayhuaman KAA, Rossi EF, Botticelli D. Influence on marginal bone levels at implants equipped with blades aiming to control the lateral pressure on the cortical bone. An experimental study in dogs. Oral Maxillofac Surg. 2024 Mar 2. doi: 10.1007/s10006-024-01228-z. Epub ahead of print. PMID: 38429433.
45. Bosshardt DD, Salvi GE, Huynh-Ba G, Ivanovski S, Donos N, Lang NP. The role of bone debris in early healing adjacent to hydrophilic and hydrophobic implant surfaces in man. Clin Oral Implants Res. 2011 Apr;22(4):357-64. doi: 10.1111/j.1600-0501.2010.02107.x. PMID: 21561477.
46. Lang NP, Salvi GE, Huynh-Ba G, Ivanovski S, Donos N, Bosshardt DD. Early osseointegration to hydrophilic and hydrophobic implant surfaces in humans. Clin Oral Implants Res. 2011 Apr;22(4):349-56. doi: 10.1111/j.1600-0501.2011.02172.x. PMID: 21561476.
47. Rossi F, Lang NP, De Santis E, Morelli F, Favero G, Botticelli D. Bone-healing pattern at the surface of titanium implants: an experimental study in the dog. Clin Oral Implants Res. 2014 Jan;25(1):124-31. doi: 10.1111/clr.12097. Epub 2013 Jan 4. PMID: 23289845.
48. Ivanoff CJ, Sennerby L, Lekholm U. Influence of mono- and bicortical anchorage on the integration of titanium implants. A study in the rabbit tibia. Int J Oral Maxillofac Surg. 1996;25:229-35.
49. Bhave SM, Chand S, Yadav L, Pal US, Mohammad S, Singh V, Singh G, Maurya H. Comparative evaluation of dental implants in posterior maxilla placed using unicortical and bicortical anchorage-A split-mouth prospective study. Natl J Maxillofac Surg. 2023 Jan-Apr;14(1):109-118. doi: 10.4103/njms.njms_7_22. Epub 2023 Apr 14. PMID: 37273433; PMCID: PMC10235748.
50. Thomé G, Caldas W, Bernardes SR, Cartelli CA, Gracher AHP, Trojan LC. Implant and prosthesis survival rates of full-arch immediate prostheses supported by implants with and without bicortical anchorage: Up to 2 years of follow-up retrospective study. Clin Oral Implants Res. 2021 Jan;32(1):37-43. doi: 10.1111/clr.13678. Epub 2020 Dec 13. PMID: 33211323.

 doi:10.20944/preprints202407.0788.v1

51. Ng P, Hu X, Wan S, Mo H, Deng F. Clinical Outcomes of Bicortical Engagement Implants in Atrophic Posterior Maxillae: A Retrospective Study with 1 to 5 Years Follow-up. Int J Periodontics Restorative Dent. 2018 September/October;38(5):e96–e104. doi: 10.11607/prd.3241. Epub 2018 Apr 20. PMID: 29677226.
52. Maló P, de Araújo Nobre M, Lopes A, Moss S. Posterior maxillary implants inserted with bicortical anchorage and placed in immediate function for partial or complete edentulous rehabilitations. A retrospective clinical study with a median follow-up of 7 years. Oral Maxillofac Surg. 2015 Mar;19(1):19-27. doi: 10.1007/s10006-014-0444-7. Epub 2014 Feb 28. PMID: 24577629.
53. Chang SH, Lin CL, Lin YS, Hsue SS, Huang SR. Biomechanical comparison of a single short and wide implant with monocortical or bicortical engagement in the atrophic posterior maxilla and a long implant in the augmented sinus. Int J Oral Maxillofac Implants. 2012 Nov-Dec;27(6):e102-11. PMID: 23189315.